

SELF-ASSEMBLY AT METAL SURFACES

J. V. Barth, H. Brune, T. Zambelli,* and K. Kern

Institut de Physique Expérimentale

Ecole Polytechnique Fédérale de Lausanne, CH-1015 Lausanne, Switzerland

**Fritz-Haber-Institut der Max-Planck-Gesellschaft*

Faradayweg 4-6, D-14195 Berlin, Germany

ABSTRACT

The recent development of temperature controlled scanning tunneling microscopy opened the door to a fascinating new world on the nanometer scale. The atomic scale information obtained provides unprecedented insight into the kinetics of surface phenomena such as epitaxial growth or chemisorption. In particular, a rich variety of surface structures could be observed, whose morphologies are determined by the self-assembly of the adsorbed particles. Temperature control allows for detailed investigations of the microscopic processes which are at the origin of the self-assembly. Some illustrative examples are discussed, particularly the initial stages in heteroepitaxial growth of metals (Ag, Cu) on fcc single crystal metal substrates with different symmetry (Pd(110), Pt(111), Ni(100)) with emphasis on the island shapes as well as a novel pattern formation in dissociative adsorption of molecular oxygen on Pt(111).

1. INTRODUCTION

In a world of continuing miniaturization, the science of nanostructures plays a vital role for the optimization of existing and the development of future materials and technologies. Extensive experimental and theoretical efforts are undertaken to explore the physical and chemical properties of materials at the nanometer scale [1]. Novel scientific approaches for the controlled formation and the characterization of nanostructured materials are in high demand. The advent of variable temperature and 4 K scanning tunneling microscopy (STM) certainly represent milestones in the development of techniques which can be used to investigate or

influence ordering processes of particles on surfaces, be it directly by manipulation of individual atoms at the lowest temperatures [2], or indirectly by exploiting the laws governing their self-assembly [3]. The objective of the present contribution is to illustrate the capabilities of variable temperature STM in the domain of nanostructuring on surfaces via self-assembly by a discussion of a few selected examples.

Firstly, we concentrate on heteroepitaxial growth of metals on single crystal transition metal substrates with different symmetry. In an experiment, where metal atoms are deposited on a surface, aggregates will evolve, corresponding to a lowering of the system's free energy [4]. However, the formation of aggregates (islands) is subjected to kinetic limitations [5], which depend on the specific characteristics of the system and can be regulated by the substrate temperature and deposition flux. Agglomeration necessitates surface diffusion of the adsorbed metal atoms, initially randomly distributed on the substrate. The average adatom diffusion length Λ_a is strongly temperature (and flux) dependent (at constant flux: $\Lambda_a \sim \exp(-\chi E^*/2kT)$, where E^* is a corresponding activation energy and χ a scaling exponent). Once a minimum number of atoms find each other, their growth becomes more likely than their dissolution and a stable nucleus forms [5, 6]. The critical number of atoms which forms a stable nucleus upon incorporation of exactly one additional atom is referred to as the critical nucleus size i , which is the temperature dependent decisive parameter for the scaling exponent χ [7]. Attachment of additional diffusing atoms leads to the growth of the nucleus. The shape of the island formed, will depend on the one hand on the substrate symmetry. It may be used to induce anisotropies in the surface diffusion and the sticking of mobile atoms to islands, respectively. On the other hand, the island shape is determined by the mobility of attached atoms along the perimeter of the islands Λ_1 , which is again temperature dependent ($\Lambda_1 \sim \exp(E^*/kT)$), and can be similarly influenced by the substrate geometry. At the lowest temperatures, where Λ_1 is very small, mechanisms with very limited edge mobility prevail, resulting in the formation of fractal islands, resembling those known from diffusion limited aggregation (DLA) studies [8] (note, however, that with all metal on metal systems investigated so far, edge mobilities in island formation never could be completely suppressed as would be the case for an ideal DLA growth). With increasing temperatures, the influence of Λ_1 becomes more pronounced, i.e., the adatom migration along island edges strongly influences the island morphology. A further parameter which influences the island shape, whose importance in heteroepitaxial growth was realized only recently, is the strain present in the islands due to the mismatch between the substrate and the adsorbate lattice. This can lead to symmetry breaking in growth and corresponding formation of ramified islands even in thermodynamic equilibrium, due to a more efficient strain relief associated with such structures.

Secondly, the application of variable temperature STM to growth processes which involve adsorption of gas molecules and surface chemical processes, will be demonstrated. With such systems, adsorbed particles do not necessarily reach the minimum of the chemisorption well directly, as opposed to the case of metal deposition. Rather, the intermediate population of metastable precursor states frequently occurs, leading to very different growth characteristics. By means of temperature controlled STM a comprehensive characterization of such processes becomes accessible, as will be demonstrated below. Additionally, it allows for an elucidation of the local chemical reactivity of the surface, which can play a decisive role in the self-assembly of the surface chemical reaction products.

2. EXPERIMENTAL

Experiments were performed in ultrahigh-vacuum chambers (base pressure $\approx 1 \times 10^{-10}$ Torr) with home-built beetle-type STMs cooled by liquid He [9, 10]. Sample preparation and characterization followed standard procedures. The data presented were obtained in the constant-current mode. Metals were deposited by vapor-phase epitaxy with commercial Knudsen cells. Oxygen was exposed by back filling the chamber. Coverages are given in terms of monolayers (ML, where 1 ML corresponds to one adsorbed metal atom or O_2 molecule per substrate atom, respectively).

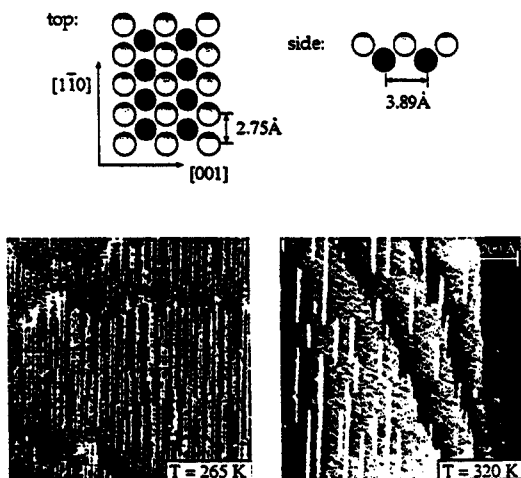


Figure 1. Model of the anisotropic Pd(110) surface and STM data of Cu islands grown on Pd(110). At $T = 265$ K monoatomic one-dimensional Cu chains forming the $[1\bar{1}0]$ channels on the substrate, whereas at $T = 320$ K two-dimensional anisotropic growth prevails ($\Theta_{Cu} \approx 0.1$ ML).

2.1. One-dimensional islands on anisotropic surfaces: Cu/Pd(110)

A conceptually simple way to synthesize islands with a desired shape is to take advantage of the anisotropy provided by a substrate with low symmetry. This can be used to obtain 1-dimensional aggregates, as demonstrated by the data reproduced in Fig. 1 for growth of Cu on a Pd(110) surface [3, 11]. For this system, the diffusion barriers along the close-packed $[1\bar{1}0]$ and open $[001]$ direction were determined by a recent detailed analysis using kinetic Monte Carlo simulations to ≈ 0.30 eV and ≈ 0.45 eV, respectively [12]. Hence surface diffusion is predominantly one-dimensional at low temperatures and monoatomic chains of Cu atoms form in the $[1\bar{1}0]$ channels of the Pd(110) substrate. The average length of these

chains decreases with deposition temperature, allowing for controlled fabrication of monoatomic wires of a desired length. The simulations revealed that the monoatomic wires even evolve in the temperature regime where cross-channel diffusion is allowed. However, anisotropic irreversible sticking of diffusing atoms to the islands must exist, i.e., atoms can only be effectively bound to an island if they are attached at the energetically favorable next-neighbor site in the $[1\bar{1}0]$ direction, whereas they are free to move if they are located in a $[1\bar{1}0]$ channel next to an island [12]. With deposition temperatures exceeding a critical temperature of ≈ 270 K, this sticking irreversibility is lifted, which results in the formation of rectangular islands, whose average width can be controlled via the temperature.

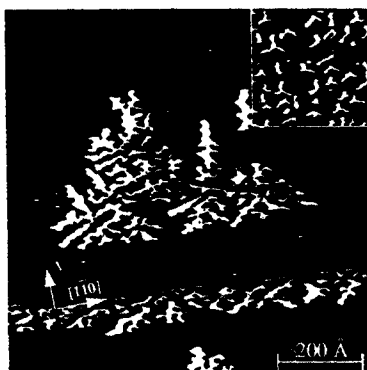


Figure 2. Dendritic islands formed in epitaxial growth of Ag on Pt(111) at 130 K and 80 K (inset); $\Theta_{\text{Ag}} = 0.12$ ML, deposition flux 1.1×10^{-3} ML/s.

2.2. Dendritic islands by kinetic limitations in growth on a trigonal surface: Ag/Pt(111)

At low temperature branched islands evolve in epitaxial metal growth on a close-packed fcc(111) metal substrate. This is demonstrated by the STM image reproduced in Fig. 2 for the Ag/Pt(111) system [13, 14]. With this system the individual Ag atoms, initially present on the surface, are mobile even at low temperatures since the energy barrier for single atom migration is small on a close-packed substrate (160 meV [6]). In the example shown, the adatom aggregation leads to formation of dendritic islands with a trigonal symmetry reflecting the threefold symmetry of the Pt(111) surface. The inset in Fig. 1 demonstrates the initial branching for small islands obtained at $T = 80$ K. These islands are Y-shaped with three branches rotated by 120° . More detailed investigations allow for the identification of the growth direction with the crystallographic $[\bar{1}\bar{1}2]$ direction [6, 15]. Therefore the Y's exclusively appear in one orientation. The larger dendrites formed at 130 K retain the preferential growth direction, which leads to an overall triangular envelope of the islands.

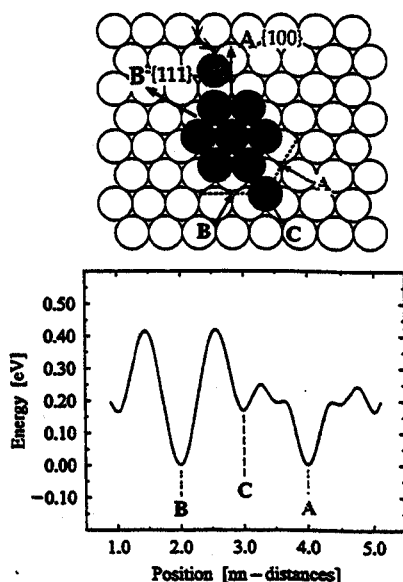


Figure 3. Model illustrating the mechanisms favoring formation of dendritic islands on a fcc(111) substrate and difference in total energy for the diffusion of a Ag atom from a corner site (C) of a Ag heptamer on Pt(111) to the two possible step types (A and B).

The basic mechanisms leading to preferential growth directions, which are linked to the substrate symmetry, are illustrated by the model and results of effective medium theory (EMT [16]) calculations shown in Fig. 3 [15]. The starting point is a stable close-packed Ag-heptamer consisting of 7 atoms located at the preferred fcc substrate hollow sites. It is important to note that there are two different step types present on an fcc(111) surface, labeled A and B in the model. The A- or B-type step forms a {100} or {111} microfacet with the underlying substrate, respectively. An atom which reaches the preferential capture site of the island, a protruding corner (site C), faces two possibilities for edge diffusion along the heptamer, leading to its attachment to an A or B type step with increased coordination and hence higher binding energy. The EMT calculations, where the energetics of these two pathways were calculated, clearly demonstrate that the energy barrier from C to A is much smaller than that from C to B leading to the preferential population of A-type sites [15]. This energy difference can be rationalized by inspection of the respective paths. Diffusing to site B involves coming very close to the energetically unfavorable top position of a substrate atom. In contrast, site A can be easily reached via diffusing over a neighboring hcp site, without completely losing the coordination to the heptamer. In a similar way, a randomly diffusing adatom occupying the same similar hcp site close to the heptamer, is attracted towards an A-

type step. This is a second reason for the directional growth. B-type steps cannot be reached in the same way. Both processes are equally important for the preferred population of A-type steps and the resulting directional growth. Nevertheless, there is a small statistical chance for an attachment of diffusing atoms at B steps. This leads to some randomness apparent in the islands. It is interesting to note, that for very low deposition rates with the same system the growth behavior changes and fractal rather than dendritic islands form [13, 14].



Figure 4. Model for edge diffusion mechanisms in epitaxial growth on a square substrate.

2.3. Strain-induced island ramification in equilibrium on a square substrate: Cu/Ni(100)

The discussion in the preceding section demonstrated that the dendritic growth of islands on a close-packed substrate is possible since kinetic limitations prevent the realization of the compact equilibrium shape. The symmetry of the fcc(111) surface plays a crucial role in this process, since it provides the possibility to reach sites with higher coordination by a single atom movement from a corner site to an edge. The anisotropy of this movement with respect to the two different types of atomic steps results in distinct growth directions. The situation is quite different for the quadratic fcc(100) substrate, as illustrated by the model in Fig. 4. Due to the substrate geometry there is no direct next-neighbor lateral binding at the island corner site and in addition, atoms arriving there face an equal choice for two diffusion processes towards similar island edges. Furthermore, once the atom is bound to the island edge, its only chance to find an energetically favorable site with higher coordination is diffusion to a kink site. Energetically favorable sites can usually not be reached by a single atom hop. From this it was inferred that in epitaxial growth on an fcc(100) square substrate a sharp transition between two growth regimes should prevail [17]: (i) at the lowest temperatures, where edge mobilities are possibly suppressed, fractal islands might form; (ii) if the temperature is high enough to allow for motions along the edge, compact islands should immediately evolve, since atoms at the edges remain mobile until the more stable kink sites

are reached. So far these ideas seem to agree with experimental evidence and exclusively compact islands have been observed in metal epitaxial growth on square substrates (e.g., [18-20]).

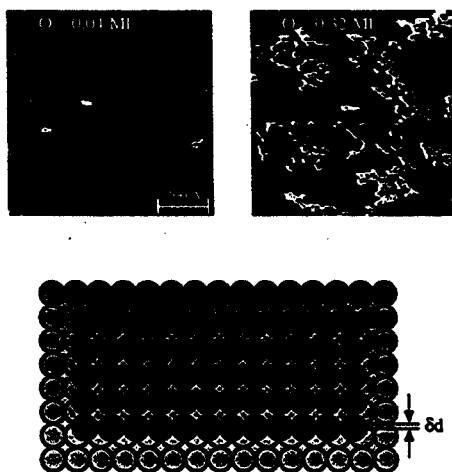


Figure 5. Island ramification in heteroepitaxial growth of Cu on a square Ni(100) substrate (deposition at 345 K, flux 1.5×10^{-3} ML/s) and ball model visualizing the local edge relaxation due to the lattice mismatch of the materials, which induces the island shape transition.

The STM data in Fig. 5 demonstrate, however, that island ramification in heteroepitaxial growth on square substrates can definitely exist even for growth at elevated temperature, where the edge mobilities are high enough to ensure equilibrium shapes. This holds for a wide range of substrate temperature (250 - 370 K) and deposition flux (6×10^{-5} - 3×10^{-2} ML/s) [21]. Moreover, a statistical analysis of the observed island shapes reveals, that the ramification is size-dependent and sets only in if the number of atoms forming Cu islands exceeds a critical value of ≈ 480 atoms, quite independent of the growth conditions. Small islands remain compact, as expected, whereas the larger ones become irregular. These findings cannot be associated with kinetic limitations in the island growth. Rather, they are rationalized as a consequence of the positive lattice mismatch of the materials (+ 2.6 %). Since the islands grow pseudomorphic in the coverage range investigated here, this mismatch creates strain within the islands. Additionally, small displacements from the Cu atoms from the ideal fourfold hollow substrate positions exist, which are assumed to be largest at the island edges, as illustrated by the model in Fig. 5, corresponding to an effective strain relieve there. The strain relieved at the island edges results in an energy gain by the island ramification, which compensates for the loss of energy due to the increased perimeters of the irregular as compared to compact islands. Indeed, these findings confirm earlier theoretical considerations [22],

where a similar strain driven, island size dependent shape transition was derived : small islands were predicted to be compact, whereas for larger islands a break of the symmetry allows for a more effective stress relaxation.

2.4. Pattern formation in precursor mediated dissociative chemisorption : $O_2/Pt(111)$

In contrast to metal deposition, for chemisorption of gases precursor states exist prior to the equilibration of the adsorbates. As a consequence the distribution of the adsorbed particles on a surface can be strongly affected by the precursor mobility on the surface, which will be in general very different from that of the final state. Dissociative adsorption of oxygen on Pt(111) proceeds via sequential population of precursor states [23-26], i.e., a physisorbed and a chemisorbed molecular oxygen species, which can be stabilized on the surface by reducing the crystal temperature to values below 30 K and 160 K, respectively. Our data show, however, in agreement with electron energy-loss spectroscopy [27] and recent STM observations [28], that for small coverages oxygen adsorbs dissociatively down to at least ≈ 95 K.

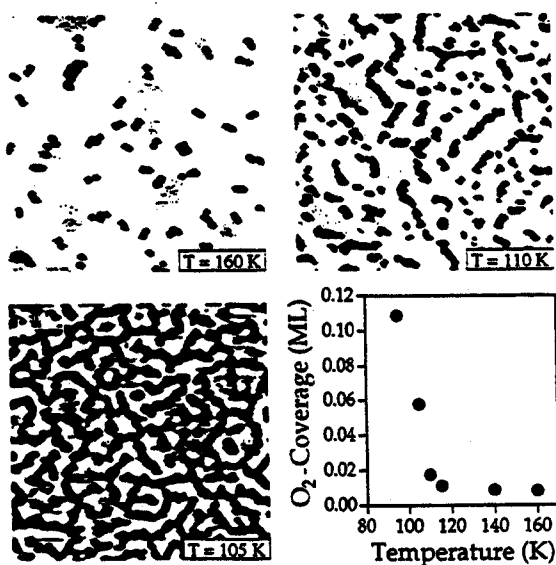


Figure 6. STM images of Pt(111), recorded after adsorption of 1 L of O_2 at the indicated temperatures and plot of the corresponding O_2 -coverages as a function of temperature.

Thermally activated surface diffusion of chemisorbed O atoms is suppressed on the time scale of the experiments at temperatures below 160 K [10] and hence the STM images reproduced in Fig. 6, recorded after exposing the Pt(111) surface to an identical dose of 1 L O_2 (1 L = 10^6 Torr s) at sample temperatures between 105 K and 160 K, reflect the distributions of adatoms right after dissociation [29]. At the highest temperature, $T = 160$ K, the O-atoms always appear as pairs (imaged as dark spots) which are randomly distributed across the surface. In agreement with previous findings, atoms in these pairs exhibit a preferential separation of twice the lattice constant, $2a = 5.6$ Å, due to non-instantaneous release of the excess energy with dissociative adsorption ('hot atom' mechanism [30]) [10]. Upon lowering the substrate temperature to 115 K, cluster formation of the oxygen pairs is predominant. At $T = 110$ K, these clusters have grown quasi-one-dimensionally along the close-packed $[1\bar{1}0]$ directions on the surface, with lengths between 10 Å and 50 Å. At 105 K the atoms are almost exclusively arranged in such chains, which are partly interconnected now forming an irregular network with about 40 Å periodicity. Oxygen islands were observed beginning with the lowest coverages and during *in situ* experiments at appropriate temperatures. These observations rule out the possibility that island formation is due to a locally enhanced sticking coefficient at the island edges. Rather, a *mobile* precursor state for the oxygen molecules occupied prior to their dissociation must be invoked to account for this process. The island formation is rationalized by the role of already chemisorbed oxygen as an active site for the dissociation of this precursor. This behavior is similar to the $O_2/Ag(110)$ system, where mobile 'hot' O_2 -precursors can be trapped by chemisorbed O_2 -molecules [31]. The oxygen coverages included in Fig. 6 indicate in agreement with earlier observations a marked increase of the sticking probability at temperatures below 120 K [26]. It is obvious that oxygen island formation and the increase of the sticking probability are directly correlated. The temperature dependence of the sticking is understood as the result of the competition between mobility, allowing to reach the active sites for equilibration, and thermal desorption of oxygen molecules from their precursor state. This mechanism is substantiated with the help of the atomic resolution STM data in Fig. 7. Initially, at 160 K, O_2 molecules may statistically dissociate and form pairs. Already at 140 K some of the precursor molecules have a chance to find their way to pairs of atoms where they dissociate (see Fig. 7). At even lower temperatures this process is more pronounced leading to the larger agglomerates. With decreasing temperature the lifetime of the precursor at the surface increases. Since the activation energy for surface diffusion is generally merely a fraction of the adsorption energy, this causes an increase of the diffusion length of the precursor on the surface. (Note that this contrasts the behavior of nonevaporating particles like the metal-on-metal systems discussed above, where the diffusion length increases with the temperature.)

The mean free path of the precursor state is determined by its mean residence time τ on the surface and its hopping rate v_{hop} on the surface, parameters determined by Arrhenius equations. The mean free path of the molecules is then given by the expression $\lambda = a/\tau v = a [v_{hop}/v_{des} \exp(E_{des}(1-\alpha)/kT)]^{1/2}$, where E_{des} is the activation energy for desorption, α the ratio between the diffusion and the desorption barrier and v_{hop} and v_{des} the corresponding prefactors. Assuming $v_{hop} \approx v_{des}$ and $\alpha \approx 0.2$, a rule of thumb in surface diffusion, this expression reduces to $\lambda \approx a \exp(2 E_{des}/5 kT)$. Taking $E_{des} = 100$ meV, which is the binding energy of physisorbed molecules [24, 32], the temperature dependence of the mean free paths matches very well the requirements for the oxygen uptake curve and the pattern formation (e.g., $\lambda \approx 20$ a, 100 a at

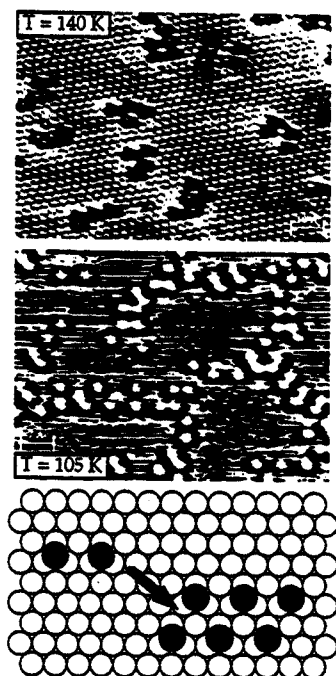


Figure 7. Atomic resolution images of oxygen islands illustrating the enhanced precursor dissociation probability near adsorbed atomic oxygen and the resulting quasi-one-dimensional growth for $T = 140$ K : small clusters form (3 L dose), $T = 105$ K : chain-shaped islands in $\langle 110 \rangle$ corresponding to strings of oxygen pairs (1 L dose) and model visualizing the directional growth of O_{ad} islands (black spheres) on Pt(111).

160 K, 100 K, respectively). The increased dissociation probability of the diffusing precursors near already chemisorbed oxygen is attributed to an increase of the adsorption energy and corresponding lowering of the activation barrier for dissociation near adsorbed oxygen atoms which leads to the formation of 4 atom-clusters and continues with the creation of chains. The quasi-one-dimensional growth of the clusters is very surprising in view of the threefold symmetry of the substrate lattice. It cannot be explained by the diffusion of the precursor alone and strongly contrasts the dendritic growth of metal islands on the same surface. It must be related to an interaction anisotropy between the atoms in the chains and the molecular precursor, which is associated with a higher chemical activity of O atoms at the chain ends due to their lower coordination to neighboring O (see model in Fig. 7).

3. CONCLUSIONS

The processes of self-assembly described above are believed to be of general importance for the synthesis of nanostructures on surfaces. The knowledge of the parameters governing the self-assembly of adsorbed particles may be transformed to obtain versatile tools for the tailoring of islands with a desired shape : for growth systems in the kinetic regime via diffusion-controlled aggregation and in the thermodynamic equilibrium regime via strain-induced island shapes, respectively. In addition we demonstrated the complexity for growth processes involving precursors and surface chemical reaction, resulting from the precursor mobility and the heterogeneity created by the reaction products. The pathways revealed have to be considered in catalytic reactions or chemical vapor deposition if diffusion lengths reach certain critical values determined by the distribution of adsorbed particles, and might be thus similarly useful for formation of nanostructures.

ACKNOWLEDGEMENTS

J.V.B. wishes to express his sincere thanks to the organizers, Profs. B. Rao, P. Jena, and S.N. Behera, for the invitation to a remarkable workshop on novel materials. The work of T.Z. was supported by the Deutscher Akademischer Austauschdienst (DAAD). Stimulating discussions with J. Wintterlin and G. Ertl are gratefully acknowledged.

References

- [1] *Physics and Chemistry of Finite Systems : From Clusters to Crystals*, Eds. P. Jena, S. N. Khanna, and B. K. Rao(Kluwer, Dordrecht, 1992).
- [2] D. M. Eigler and E. K. Schweizer, *Nature* **344**, 524 (1990).
- [3] H. Röder, E. Hahn, H. Brune, J. P. Bucher, and K. Kern, *Nature* **366**, 141 (1993).
- [4] R. Kern, G. L. Gay, and J. J. Metois, in *Current Topics in Material Science* Vol. 3, E. Kaldis, Eds.(North-Holland, 1979), pp. 134.
- [5] J. A. Venables, G. D. T. Spiller, and M. Hanbücken, *Rep. Prog. Phys.* **47**, 399 (1984).
- [6] H. Brune, H. Röder, C. Borragno, and K. Kern, *Phys. Rev.Lett.* **73**, 1955 (1994).
- [7] J. Villain, A. Pimpinelli, L. Tang, and D. Wolf, *J. Phys.(Paris) I* **2**, 2107 (1992).
- [8] T. A. Witten and L. M. Sander, *Phys. Rev. B* **27**, 5686(1983).
- [9] H. Brune, H. Röder, K. Bromann, and K. Kern, *Thin Sol. Films* **264**, 230 (1995).

- [10] J. Wintterlin, R. Schuster, and G. Ertl, *Phys. Rev. Lett.* **77**, 123 (1996).
- [11] J. P. Bucher, E. Hahn, P. Fernandez, C. Massobrio, and K. Kern, *Europhys. Lett.* **27**, 473 (1994).
- [12] Y. Li, M. C. Bartelt, J. W. Evans, N. Waelchli, E. Kampshoff, K. Kern, and A. dePristo (1997); submitted.
- [13] H. Brune, C. Romainczyk, H. Röder, and K. Kern, *Nature* **369**, 469 (1994).
- [14] H. Brune, K. Bromann, K. Kern, J. Jacobsen, P. Stoltze, K. Jacobsen and J. Nørskov, *Mat. Res. Soc. Symp. Proc.* **407**, 379 (1996).
- [15] H. Brune, K. Bromann, K. Kern, J. Jacobsen, P. Stoltze, K. Jacobsen, and J. Nørskov, *Surf. Sci. Lett.* **349**, L115(1996).
- [16] K. W. Jacobsen, J. K. Nørskov, and M. J. Puska, *Phys. Rev. B* **35**, 7423 (1987).
- [17] Z. Zhang, X. Chen, and M. G. Lagally, *Phys. Rev. Lett.* **73**, 1829 (1994).
- [18] E. Kopatzki, S. Günther, W. Nichtl-Pecher, and R. J. Behm, *Surf. Sci.* **284**, 154 (1993).
- [19] J. A. Stroscio, D. T. Pierce, and R. A. Dragoset, *Phys. Rev. Lett.* **70**, 3615 (1995).
- [20] E. Hahn, E. Kampshoff, N. Wälchli, and K. Kern, *Phys. Rev. Lett.* **74**, 1803 (1995).
- [21] B. Müller, L. Nedelmann, B. Fischer, H. Brune, J.V. Barth, and K. Kern, *Phys. Rev. Lett.* (1997); submitted.
- [22] J. Tersoff and R. M. Tromp, *Phys. Rev. Lett.* **70**, 2782 (1993).
- [23] A. C. Luntz, M. D. Williams, and D. S. Bethune, *J. Chem. Phys.* **89**, 4381 (1988).
- [24] A. C. Luntz, J. Grimblot, and D. E. Fowler, *Phys. Rev. B* **39**, 12903 (1989).
- [25] W. Wurth, J. Stöhr, P. Feulner, X. Pan, K. R. Bauchspiess, Y. Baba, E. Hudel, G. Rucker, and D. Menzel, *Phys. Rev. Lett.* **65**, 2426 (1990).
- [26] C. T. Rettner and C. B. Mullins, *J. Chem. Phys.* **94**, 1626 (1991).
- [27] H. Steininger, S. Lehwald, and H. Ibach, *Surf. Sci.* **123**, 1 (1982).
- [28] B. C. Stipe, M. A. Rezaei, W. Ho, S. Gao, M. Persson, and B. I. Lundqvist, (1997); submitted.

- [29] T. Zambelli, J. V. Barth, J. Winterlin, and G. Ertl, (1997); submitted.
- [30] H. Brune, J. Winterlin, R. J. Behm, and G. Ertl, *Phys. Rev. Lett.* **68**, 624 (1992).
- [31] J. V. Barth, T. Zambelli, J. Winterlin, and G. Ertl, *Chem. Phys. Lett.* (1997); in press.
- [32] A. N. Ansykhovich, V. A. Ukraintsev, and I. Harrison, *Surf. Sci.* **347**, 303 (1996).